Full-gap superconductivity in noncentrosymmetric Re_6Zr, $Re_{27}Zr_5$, and $Re_{24}Zr_5$

K. Matano,[1] R. Yatagai,[1] S. Maeda,[1] and Guo-qing Zheng[1,2]

[1]*Department of Physics, Okayama University, Okayama 700-8530, Japan*

[2]*Institute of Physics, Chinese Academy of Sciences, and Beijing National Laboratory for Condensed Matter Physics, Beijing 100190, China*

(Received 12 April 2016; revised manuscript received 25 November 2016; published 21 December 2016)

The noncentrosymmetric superconductor Re_6Zr has attracted much interest for its possible unconventional superconducting state with broken time-reversal symmetry. Here we report $^{185/187}$Re nuclear quadrupole resonance measurements on Re_6Zr ($T_c = 6.72$ K) and the isostructural compounds $Re_{27}Zr_5$ ($T_c = 6.53$ K) and $Re_{24}Zr_5$ ($T_c = 5.00$ K). The nuclear spin-lattice relaxation rate $1/T_1$ shows a coherence peak below T_c and decreases exponentially at low temperatures in all three samples. The superconducting gap Δ derived from the $1/T_1$ data is $2\Delta = 3.58k_BT_c$, $3.55k_BT_c$, and $3.51k_BT_c$ for Re_6Zr, $Re_{27}Zr_5$, and $Re_{24}Zr_5$, respectively, which is close to the value of $3.53k_BT_c$ expected for weak-coupling superconductivity. These data suggest conventional s-wave superconductivity with a fully opened gap in this series of compounds.

DOI: 10.1103/PhysRevB.94.214513

I. INTRODUCTION

Superconductors with broken symmetries, such as broken time-reversal symmetry [1] or broken spin-rotation symmetry [2], have attracted great attention. In particular, the role of the crystal structure in the emergence of unconventional superconducting states has been studied extensively in recent years.

In superconductors with an inversion center in the crystal structure, either an even-parity spin-singlet or an odd-parity spin-triplet superconducting state is realized. However, in noncentrosymmetric superconductors, a parity-mixed superconducting state is allowed and an antisymmetric spin-orbit coupling (ASOC) interaction is induced [3–5]. The parity-mixing extent is determined by the strength of the ASOC.

Indeed, some noncentrosymmetric superconductors show novel features. For example, isostructural Li_2Pd_3B and Li_2Pt_3B show contrasting behaviors. Li_2Pd_3B exhibits conventional BCS-type properties [6], while Li_2Pt_3B is a spin-triplet dominant superconductor [7] with nodes in the gap function [7,8]. In this case, a different ASOC due to differences in peculiar crystal structure distortion and atomic number were responsible for the different superconducting states [9]. After the discovery of spin-triplet superconductivity in Li_2Pt_3B, extensive studies have been performed to search for novel superconductivity in noncentrosymmetric superconductors containing heavy elements such as $Mg_{10+x}Ir_{19-y}B$ [10], BiPd [11], and ScIrP [12], but parity-mixing is found to be weak [13,14], due to a crystal structure that does not lead to strong ASOC enhancement.

Recently, more novel properties were reported in some noncentrosymmetric superconductors. For example, a small internal magnetic field was detected below T_c in noncentrosymmetric $LaNiC_2$, which was interpreted as due to a breaking of time-reversal symmetry in the superconducting state [1], although a relation between the breaking of inversion symmetry and time-reversal symmetry is unclear.

Noncentrosymmetric Re_6Zr is a new candidate for a time-reversal symmetry-breaking superconductor. Re_6Zr has an α-Mn type cubic crystal structure with space group $I\bar{4}3m$ [15] and a large upper critical field close to the Pauli limit [16]. Figure 1 shows the α-Mn type crystal structure, which has four independent crystallographic sites Mn I: $2a$ (Wyckoff), $\bar{4}3m$ (Hermann-Mauguin), Mn II: $8c,3m$, Mn III: $24g_1,m$, and Mn IV: $24g_2,m$ [17]. Among them, only the Mn I ($2a,\bar{4}3m$) site has an inversion center. An internal magnetic field was detected in the superconducting state by muon spin relaxation or rotation (μSR) measurements [16]. The result was ascribed to broken time-reversal symmetry in the superconducting state. It is known that a chiral p-wave state or a chiral d-wave state can produce a tiny internal magnetic field [18,19].

In order to investigate the gap structure, we performed nuclear quadrupole resonance (NQR) measurements on Re_6Zr, and the isostructural compounds $Re_{27}Zr_5$ and $Re_{24}Zr_5$. These compounds have an α-Mn type crystal structure but with different superconducting transition temperatures, with $Re_{24}Zr_5$ being stoichiometric. The NQR measurement performed at zero magnetic field is one of the most powerful methods for the study of the superconducting gap symmetry. We find that all the three compounds show superconducting properties consistent with a conventional BCS gap symmetry.

II. EXPERIMENT

The polycrystalline samples of Re_6Zr, $Re_{27}Zr_5$, and $Re_{24}Zr_5$ in this study were synthesized by the arc-melting method. The Re (99.99%) and Zr (99.9%) were arc melted under an argon atmosphere. The difference in mass before and after the melting was less than 1% for all samples. The melted ingots were crushed into powders for x-ray diffraction (XRD) and NQR measurements. The Cu $K\alpha$ radiation is used for the XRD measurements. The T_c was determined by measuring the ac susceptibility using the *in situ* NQR coil. A standard phase-coherent pulsed NMR spectrometer was used to collect data. The nuclear spin-lattice relaxation rate was measured by using a single saturation pulse. The spin echo was observed with a sequence of $\pi/2$ pulse (4 μs)–30 μs–π pulse (8 μs).

III. RESULTS AND DISCUSSIONS

Figure 2 shows the XRD patterns and the ac susceptibility results for Re_6Zr, $Re_{27}Zr_5$, and $Re_{24}Zr_5$. The lattice constant a is 9.714 Å for Re_6Zr, which is a little shorter than the reported value of 9.698 Å [15]. The T_c for Re_6Zr is 6.72 K,

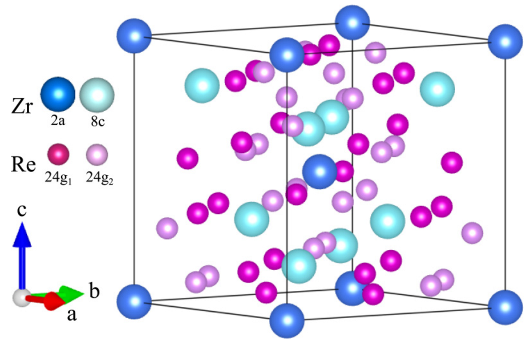

FIG. 1. Crystal structure of α-Mn type Re-Zr system. It is a cubic structure with space group $I\bar{4}3m$.

which is very close to 6.75 K reported in Ref. [16]. The obtained lattice constant and T_c are shown in Table I. For Re_6Zr and $Re_{27}Zr_5$, the XRD patterns can be fitted by the Rietveld method. For $Re_{24}Zr_5$, some unidentified peaks are observed. The linewidth increases with increasing Zr composition, which suggests that impurities or crystal distortions increase with increasing Zr composition. In the ac susceptibility for $Re_{24}Zr_5$, a small shoulder can be seen around T_c, which is likely attributable to the sample inhomogeneity. A similar result has been reported in Nb-Re systems [20]. In α-Mn type systems, $Re_{24}Zr_5$ is stoichiometric, while Re_6Zr and $Re_{27}Zr_5$ are nonstoichiometric with Re-rich compositions. In the Re_xZr_{1-x} binary phase diagram [21], a single phase α-Mn structure can be obtained only in a narrow range with $0.82 \leqslant x \leqslant 0.87$. The Re-to-Zr ratio is 82.8:17.2 for stoichiometric $Re_{24}Zr_5$, which is quite close to the limit to obtain a single phase. On the other hand, the Re-to-Zr ratio is 84.4:15.6 for $Re_{27}Zr_5$ and 85.7:14.3 for Re_6Zr. As seen in Fig. 2, the stoichiometric $Re_{24}Zr_5$ compound showed a small amount of additional peaks in the XRD chart, which is likely due to the fact that the $Re_{24}Zr_5$ is close to the phase boundary.

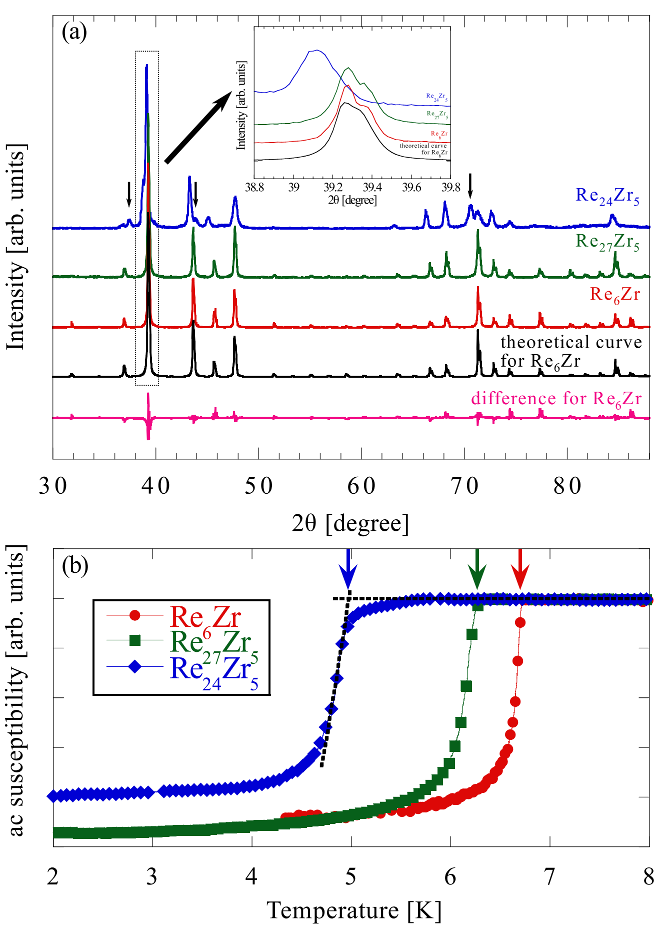

FIG. 2. (a) XRD patterns for Re_6Zr, $Re_{27}Zr_5$, and $Re_{24}Zr_5$. The theoretical curve and the differences between the theoretical curve and the observed XRD are obtained by the Rietveld method. Arrows indicate unidentified peaks. For clarity, in the inset we show the enlarged part in the range of 38.8°–39.8°. (b) ac susceptibility measured using the *in situ* NQR coil at zero magnetic field. The arrows indicate T_c for each sample.

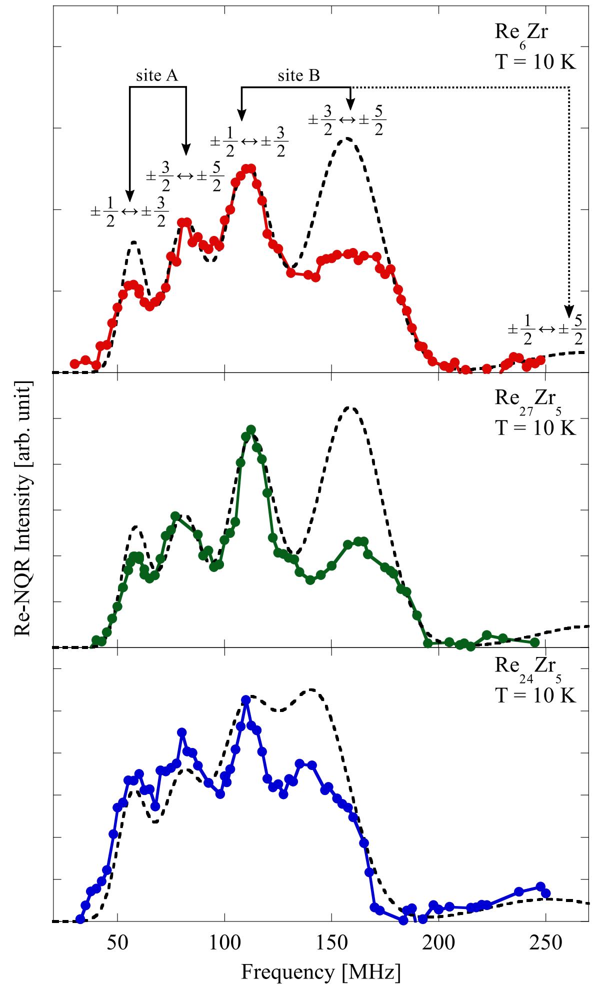

FIG. 3. $^{185/187}$Re -NQR spectrum of Re_6Zr, $Re_{27}Zr_5$, and $Re_{24}Zr_5$ measured at $T = 10$ K. Dotted curves are the theoretical simulations (see text).

Figure 3 shows the $^{185/187}$Re -NQR spectra at $T = 10$ K for the three samples. Four peaks were observed for all samples. The Re nuclei have a spin $I = \frac{5}{2}$, which will result in two transitions. In Re-Zr systems with an α-Mn type structure, the unit cell has 58 atoms that are distributed into two Zr sites ($2a$,$8c$) and two Re sites ($24g_1$,$24g_2$) [22]. Furthermore,

TABLE I. Crystal structure, the NQR parameters for ^{187}Re, and the superconductivity parameters for Re_6Zr, $Re_{27}Zr_5$, and $Re_{24}Zr_5$.

	Re_6Zr ($Re_{30}Zr_5$)		$Re_{27}Zr_5$		$Re_{24}Zr_5$	
Lattice constant (Å)	9.714		9.726		9.762	
2Δ ($k_B T_c$)	3.58		3.55		3.51	
T_c (K)	6.72		6.53		5.00	
Site	A	B	A	B	A	B
ν_Q (MHz)	42	84	42	83	42	75
η	0.6	0.6	0.6	0.6	0.6	0.7
FWHM ($\pm\frac{1}{2} \leftrightarrow \pm\frac{3}{2}$) (MHz)	13	25	14	20	16	23
FWHM ($\pm\frac{3}{2} \leftrightarrow \pm\frac{5}{2}$) (MHz)	19	36	24	34	28	37

Re has two isotopes ^{185}Re (natural abundance 37.5%) and ^{187}Re (62.5%). As a result, eight peaks for this compound are expected, in principle. However, the difference in the nuclear quadrupole moment Q of ^{185}Re (2.7×10^{-24} cm^2) and ^{187}Re (2.6×10^{-24} cm^2) is only 4%, which leads to the inability of distinguishing ^{185}Re from ^{187}Re in the broad spectra and thus only four peaks were observed. As can be seen in Fig. 3, only the uppermost peak varies upon changing the Re-Zr composition ratio. By a theoretical simulation (see below), we assigned the lower two peaks to site A and the upper two peaks to site B. At the moment, it is unclear which site (A or B) corresponds to which Re site in the crystal structure. The Hamiltonian for the quadrupole interaction is

$$\mathscr{H} = \frac{\nu_Q}{6}\left\{(3I^2 - \vec{I}^2) + \frac{\eta}{2}(I_+^2 + I_-^2)\right\}. \tag{1}$$

Here, ν_Q and η are defined as

$$\nu_Q \equiv \nu_z = \frac{3}{2I(2I-1)h}e^2 Q \frac{\partial^2 V}{\partial z^2}, \tag{2}$$

$$\eta = \frac{|\nu_x - \nu_y|}{\nu_z}, \tag{3}$$

with $\frac{\partial^2 V}{\partial \alpha^2}$ ($\alpha = x,y,z$) being the electric field gradient at the position of the nucleus. In the simulations, a Gaussian function $\exp\{-(f/2\delta)^2\}$ is convoluted, where f is the frequency and δ is related to the full width at half maximum (FWHM) of the transition line as FWHM $= 2\delta\sqrt{2\ln(2)}$. The ν_Q and η were treated as parameters. The intensity ratio of each peak depends on η. With the parameters listed in Table I, we are able to reproduce the experimental results as seen in Fig. 3. We note that ν_Q or the FWHM is proportional to Q, so the value for ^{185}Re ($Q = 2.7\times10^{-24}$ cm^2) is 1.04 times the value for ^{187}Re ($Q = 2.6\times10^{-24}$ cm^2). The intensity for the uppermost peak does not agree with the simulation, probably due to a worse quality factor of the coil in this frequency range. In the case of large η, a signal from the forbidden transitions ($\pm\frac{1}{2} \leftrightarrow \pm\frac{5}{2}$) is expected. Indeed, we detected such signals in the frequency range above 200 MHz, as seen in Fig. 3.

Figure 4 shows the temperature dependence of $1/T_1$ of $^{185/187}$Re-NQR, which was measured at the $1\nu_Q$ ($\pm\frac{1}{2} \leftrightarrow \pm\frac{3}{2}$) transition of site B. The nuclear magnetization decay curve for each compound is well fitted to the theoretical formula for different η [23],

$$\mathrm{Re_6Zr}: \frac{M_0 - M(t)}{M_0} = 0.163\exp\left(-\frac{3.00t}{T_1}\right) + 0.837\exp\left(-\frac{8.52t}{T_1}\right), \tag{4}$$

$$\mathrm{Re_{27}Zr_5}: \frac{M_0 - M(t)}{M_0} = 0.170\exp\left(-\frac{3.00t}{T_1}\right) + 0.830\exp\left(-\frac{8.42t}{T_1}\right), \tag{5}$$

$$\mathrm{Re_{24}Zr_5}: \frac{M_0 - M(t)}{M_0} = 0.187\exp\left(-\frac{3.00t}{T_1}\right) + 0.813\exp\left(-\frac{8.23t}{T_1}\right), \tag{6}$$

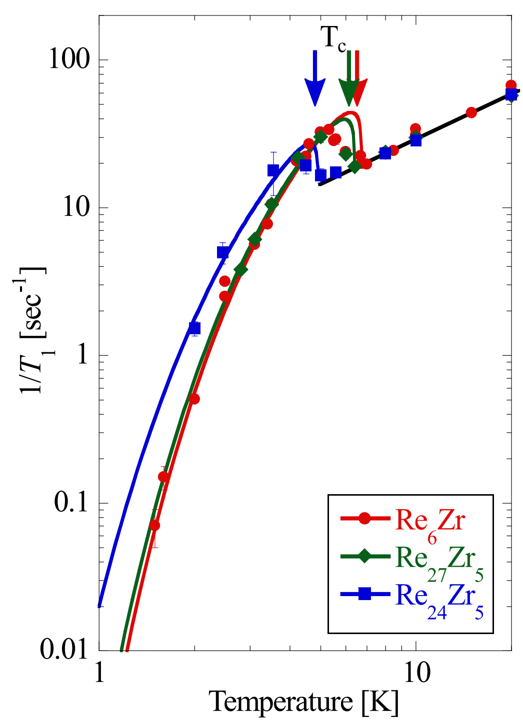

FIG. 4. Temperature dependence of the spin-lattice relaxation rate $1/T_1$ measured by NQR. The straight line above T_c represents the T_1T = const relation. The solid curve below T_c is a calculation assuming the s-wave gap function (see text).

where M_0 is the nuclear magnetization in the thermal equilibrium and $M(t)$ is the nuclear magnetization at a time t after the saturating pulse. We have confirmed that T_1 measured at the $\pm\frac{3}{2} \leftrightarrow \pm\frac{5}{2}$ transition gives the same value. The recovery curve can be fitted with a single T_1 component below and above T_c, which indicates that the macroscopic phase separation in the sample is small, if any. As seen in the figure, $1/T_1$ varies in proportion to the temperature (T) above T_c for all samples, as expected for conventional metals, indicating no electron-electron interaction. Below T_c, $1/T_1$ shows a coherence peak (Hebel-Slichter peak) expected for an s-wave superconducting state. The $1/T_{1S}$ in the superconducting state is expressed as

$$\frac{T_{1N}}{T_{1S}} = \frac{2}{k_B T}\int\left(1+\frac{\Delta^2}{EE'}\right)N_S(E)N_S(E') \times f(E)[1-f(E')]\delta(E-E')dEdE', \quad (7)$$

where $1/T_{1N}$ is the relaxation rate in the normal state, $N_S(E)$ is the superconducting density of states (DOS), $f(E)$ is the Fermi distribution function, and $C = 1 + \frac{\Delta^2}{EE'}$ is the coherence factor. To perform the calculation of Eq. (7), we follow Hebel to convolute $N_S(E)$ with a broadening function $B(E)$ [24], which is approximated by a rectangular function centered at E with a height of $1/2\delta$. The solid curve below T_c shown in Fig. 4 is a calculation with $2\Delta = 3.58k_BT_c$, $b \equiv \delta/\Delta(0) = 0.030$ for Re_6Zr, $2\Delta = 3.55k_BT_c$, $b = 0.058$ for $Re_{27}Zr_5$, and $2\Delta = 3.51k_BT_c$, $b = 0.107$ for $Re_{24}Zr_5$. The curve fits the experimental data reasonably well. The parameter 2Δ is close to the BCS value of $3.53k_BT_c$. This result indicates an isotropic superconducting gap in these compounds. A similar conclusion was drawn by a recent London penetration depth measurement for Re_6Zr [25].

Our result is inconsistent with a time-reversal symmetry-broken superconducting state such as $d + id$ or $p + ip$ where the coherence peak will be absent. We note that inconsistent results from different probes have been reported in $LaNiC_2$, $PrPt_4Ge_{12}$, and the locally noncentrosymmetric superconductor SrPtAs that has an inversion center in a whole unit cell but not within a single layer. In these samples, time-reversal symmetry breaking was suggested by μSR [1,19,26], but an s-wave superconductivity was confirmed by NQR/NMR measurements [27–29]. In these materials, breaking of time-reversal symmetry has not been observed, except for μSR.

IV. SUMMARY

In summary, we have performed $^{185/187}$Re -NQR measurements on the noncentrosymmetric superconductors Re_6Zr, $Re_{27}Zr_5$, and $Re_{24}Zr_5$. The T-linear behavior of the nuclear spin-lattice relaxation rate $1/T_1$ above T_c indicates the absence of spin correlations. The $1/T_1$ shows a Hebel-Slichter peak just below T_c and decreases exponentially at low temperatures for all samples, which suggests that the α-Mn type Re-Zr system is in an s-wave fully gapped superconducting state, which is inconsistent with a time-reversal symmetry-breaking state such as $d + id$ or $p + ip$.

ACKNOWLEDGMENT

This work was supported by Research Grant No. JP15H05852 (Innovative Areas "Topological Materials Science") from MEXT and Grant No. JP16H04016 from JSPS.

[1] A. D. Hillier, J. Quintanilla, and R. Cywinski, Phys. Rev. Lett. **102**, 117007 (2009).
[2] K. Matano, M. Kriener, K. Segawa, Y. Ando, and G.-q. Zheng, Nat. Phys. **12**, 852 (2016).
[3] L. P. Gor'kov and E. I. Rashba, Phys. Rev. Lett. **87**, 037004 (2001).
[4] P. A. Frigeri, D. F. Agterberg, A. Koga, and M. Sigrist, Phys. Rev. Lett. **92**, 097001 (2004).
[5] P. A. Frigeri, D. F. Agterberg, and M. Sigrist, New J. Phys. **6**, 115 (2004).
[6] M. Nishiyama, Y. Inada, and G.-q. Zheng, Phys. Rev. B **71**, 220505 (2005).
[7] M. Nishiyama, Y. Inada, and G.-q. Zheng, Phys. Rev. Lett. **98**, 047002 (2007).
[8] H. Q. Yuan, D. F. Agterberg, N. Hayashi, P. Badica, D. Vandervelde, K. Togano, M. Sigrist, and M. B. Salamon, Phys. Rev. Lett. **97**, 017006 (2006).
[9] S. Harada, J. J. Zhou, Y. G. Yao, Y. Inada, and G.-q. Zheng, Phys. Rev. B **86**, 220502 (2012).
[10] T. Klimczuk, Q. Xu, E. Morosan, J. D. Thompson, H. W. Zandbergen, and R. J. Cava, Phys. Rev. B **74**, 220502 (2006).
[11] B. Joshi, A. Thamizhavel, and S. Ramakrishnan, Phys. Rev. B **84**, 064518 (2011).
[12] Y. Okamoto, T. Inohara, Y. Yamakawa, A. Yamakage, and K. Takenaka, J. Phys. Soc. Jpn. **85**, 013704 (2016).
[13] K. Tahara, Z. Li, H. X. Yang, J. L. Luo, S. Kawasaki, and G.-q. Zheng, Phys. Rev. B **80**, 060503 (2009).
[14] K. Matano, S. Maeda, H. Sawaoka, Y. Muro, T. Takabatake, B. Joshi, S. Ramakrishnan, K. Kawashima, J. Akimitsu, and G.-q. Zheng, J. Phys. Soc. Jpn. **82**, 084711 (2013).
[15] B. Matthias, J. Phys. Chem. Solids **19**, 130 (1961).
[16] R. P. Singh, A. D. Hillier, B. Mazidian, J. Quintanilla, J. F. Annett, D. M. Paul, G. Balakrishnan, and M. R. Lees, Phys. Rev. Lett. **112**, 107002 (2014).
[17] D. Hobbs, J. Hafner, and D. Spišák, Phys. Rev. B **68**, 014407 (2003).
[18] A. P. Mackenzie and Y. Maeno, Rev. Mod. Phys. **75**, 657 (2003).
[19] P. K. Biswas, H. Luetkens, T. Neupert, T. Stürzer, C. Baines, G. Pascua, A. P. Schnyder, M. H. Fischer, J. Goryo, M. R. Lees, H. Maeter, F. Brückner, H.-H. Klauss, M. Nicklas, P. J. Baker, A. D. Hillier, M. Sigrist, A. Amato, and D. Johrendt, Phys. Rev. B **87**, 180503 (2013).
[20] J. Chen, L. Jiao, J. L. Zhang, Y. Chen, L. Yang, M. Nicklas, F. Steglich, and H. Q. Yuan, Phys. Rev. B **88**, 144510 (2013).
[21] E. M. Savitskii, M. A. Tylkina, and I. A. Tsyganova, Sov. J. At. Energy **7**, 724 (1961).
[22] J.-M. Joubert and M. Phejar, Prog. Mater. Sci. **54**, 945 (2009).
[23] J. Chepin and J. H. Ross, Jr., J. Phys.: Condens. Matter **3**, 8103 (1991).
[24] L. C. Hebel, Phys. Rev. **116**, 79 (1959).

[25] M. A. Khan, A. B. Karki, J. C. Prestigiacomo, T. Samanta, D. Browne, S. Stadler, I. Vekhter, P. W. Adams, A. Pandey, R. Prozorov, S. Teknowijoyo, K. Cho, D. E. Graf, and D. P. Young, Phys. Rev. B **94**, 144515 (2016).

[26] A. Maisuradze, W. Schnelle, R. Khasanov, R. Gumeniuk, M. Nicklas, H. Rosner, A. Leithe-Jasper, Y. Grin, A. Amato, and P. Thalmeier, Phys. Rev. B **82**, 024524 (2010).

[27] Y. Iwamoto, Y. Iwasaki, K. Ueda, and T. Kohara, Phys. Lett. A **250**, 439 (1998).

[28] F. Kanetake, H. Mukuda, Y. Kitaoka, K. ichi Magishi, H. Sugawara, K. M. Itoh, and E. E. Haller, J. Phys. Soc. Jpn. **79**, 063702 (2010).

[29] K. Matano, K. Arima, S. Maeda, Y. Nishikubo, K. Kudo, M. Nohara, and G.-q. Zheng, Phys. Rev. B **89**, 140504 (2014).